

Electro-oxidation of methanol and ethanol using a Pt–RuO₂/C composite prepared by the sol–gel technique and supported on boron-doped diamond

H.B. Suffredini^a, V. Tricoli^b, N. Vatisstas^b, L.A. Avaca^{a,*}

^a Instituto de Química de São Carlos, Universidade de São Paulo, C.P. 780, 13560-970 São Carlos, SP, Brazil

^b Dipartimento di Ingegneria Chimica, Università di Pisa, Via Diotisalvi 2, 56126 Pisa, Italy

Received 3 August 2005; received in revised form 22 September 2005; accepted 26 September 2005

Available online 22 November 2005

Abstract

A detailed description of the preparation, characterization and electrochemical performance towards methanol and ethanol oxidation in acid medium of a platinum–ruthenium oxide carbon powder composite is presented here. The composite was prepared by the sol–gel technique and fixed on the surface of a boron-doped diamond (BDD) electrode. The physical characterization by XRD and EDX revealed the crystalline nature of the catalysts particles having an average size of 7.2 nm and a mass ratio of practically 1:1 for Pt and Ru, in accordance with the preparation conditions. Initial electrochemical experiments using also glassy carbon as the substrate for the composite showed that BDD has a superior performance, probably related to the very low capacitive currents of that material. The oxidation of methanol and ethanol in H₂SO₄ solutions was studied by cyclic voltammetry, Tafel plots and chronoamperometry and the results were compared to those obtained using a commercial Pt/C powder composite under the same conditions. In all cases, the Pt–RuO₂/C composite showed larger anodic current densities and increased stability than the other material thus confirming the suitability of the simple and straightforward preparation technique for the catalysts.

© 2005 Elsevier B.V. All rights reserved.

Keywords: Modified carbon powder electrodes; Methanol electro-oxidation; Ethanol electro-oxidation; Boron-doped diamond; Fuel cells; Sol–gel

1. Introduction

Platinum–ruthenium carbon powder composites with different compositions have received attention in the last years as high specific surface anodes to be used in direct alcohol fuel cells [1–10]. Different techniques have been proposed to effectively disperse such catalysts on the carbon black powder substrate, such as the use of specific organo-metallic precursors [11], ultrasonic dispersion [12] or the preparation and deposition of special colloidal solutions [13,14].

The sol–gel coating technique, mainly used for flat surface substrates [15–17], has been recently adapted by Suffredini et al. [18] to easily prepare electrochemically active Pt–RuO₂/C electrodes. The experimental results obtained with these composites supported on glassy carbon (GC) have shown a higher

activity toward methanol electro-oxidation than the commercial state-of-art catalysts with similar Pt–Ru loading. It should be stressed here than glassy carbon (GC) substrates exhibit good stability, as opposed to other electrode materials like titanium and gold that form oxides at high anodic potentials.

Meanwhile, an innovative material, the boron-doped diamond (BDD), has been recently proposed as support for the electrochemical characterization of the chemically and electrochemically deposited platinum particles [19]. The BDD specific properties are due to its allotropic form respect to the pyrolytic graphite and vitreous carbon [20]. It shows a very large electrochemical potential window [21–23] and consequently a low background current is expected when BDD is used as support of the prepared Pt–RuO₂ composite. This characteristic is accompanied by enhanced mechanical stability and high corrosion resistance even when the electrode is subjected to high current density [24,25]. Moreover, a considerable reduction of its charge transfer resistance can be obtained by a cathodic polarization pre-treatment [26].

* Corresponding author. Tel.: +55 16 3373 9943; fax: +55 16 3373 9943.
E-mail address: avaca@iqsc.usp.br (L.A. Avaca).

Thus, the aims of this work are: (i) to use BDD as the substrate of a Pt–RuO₂/C composite electrode prepared by the sol–gel technique for the oxidation of methanol and ethanol in acid solution and to compare its performance with a commercial Pt/C powder; (ii) to extend the electrochemical characterization thereof using cyclic voltammetry, chronoamperometry and Tafel plots and (iii) to further characterize the physical structure of the Pt–RuO₂/C composite catalyst using XRD and EDX techniques.

2. Experimental

2.1. Reagents and apparatus

All electrochemical experiments were performed at room temperature in a Pyrex[®] glass cell provided with three electrodes. The reference electrode was a hydrogen system in the same solution (HESS) and the auxiliary was a 2 cm² Pt foil. The boron-doped diamond substrate was purchased from the Centre Suisse d'Electronique et de Microtechnique SA (CSEM), Neuchâtel, Switzerland. This material was prepared using the hot filament chemical vapor deposition (HF-CVD) technique with a filament temperature in the range 2440–2560 °C and a gaseous mixture containing methane, H₂ and trimethylboron. The final boron content was of the order of 4500–5000 ppm. The preparation procedure of the working electrode is explained in the next two subsections (Sections 2.2 and 2.3). The supporting electrolyte was a 0.5 mol dm⁻³ H₂SO₄ solution (Merck[®]) also containing 1.0 mol dm⁻³ methanol or ethanol (Synth[®]). The electrochemical measurements were carried out using an EG&G Princeton PAR Potentiostat/Galvanostat model 273A. The X-ray diffraction (XRD) analysis of the composite was performed on a Rigaku Rotoflex RU 200B with the Cu K α radiation. A Link Analytical QX-2000 microanalyzer was used to perform energy dispersive X-ray (EDX) analysis of the composite.

Two organo-metallic sol–gel solutions of Pt(II) and Ru(III) and carbon black powder are required for the production of the Pt–RuO₂/C composite. The platinum solution was prepared adding 0.0099 g of the Pt(II) acetylacetonate (Aldrich[®]) to 25 cm³ of a liquid mixture constituted by ethanol (Synth[®] 98°) and acetic acid (Merck[®] P.A.) 3:2 (v/v) while the ruthenium solution was prepared using the same procedure but adding 0.0098 g of the Ru(III) acetylacetonate (Aldrich[®]). The sol–gel solutions were subjected to an ultrasonic treatment (Thornton[®] Sonicator) for 5 min (homogenization step). The final concentration of these two organo-metallic solutions was 1.0 \times 10⁻³ mol dm⁻³. The carbon black powder was a Vulcan[®] XC72R. A 5% commercial Nafion[®] solution (5 wt% in low aliphatic alcohols) was purchased from Aldrich[®]. For comparative experiments, a commercial Pt/C (Etek Inc., USA) powder containing 10% of platinum was also used.

2.2. Composite preparation

The composite containing Pt, Ru and C was prepared using a fixed proportion of metals (50% Pt–50% Ru, w/w) and the Vulcan[®] XC72R carbon powder as the substrate. The total

catalyst load was fixed in 10% w/w, with respect to the carbon powder. These deposits were made by a sol–gel technique using the organo-metallic solutions described in the previous section.

The deposits were made according to Ref. [18]. Thus, the dry carbon powder (0.13 g) was placed in a beaker and a small amount of the mixed organo-metallic solutions (1–2 cm³), was added to the powder, thereby producing a “black mud” without excess of liquid. After the quasi-total evaporation of the liquid in the “black mud” (at room temperature) further amounts of 1 cm³ were added. This procedure (polymerization step) was repeated until reaching 10% of total catalysts load. The carbon powder impregnated with the organo-metallic compounds was then subjected to a thermal treatment at 400 °C for 1 h under argon atmosphere. The final system was a composite containing Pt, Ru and C.

2.3. Anchoring of the composite on the BDD substrate

Both, the composite containing Pt, Ru and C and the commercial Pt/C powder were fixed onto the surface of a BDD electrode following the procedure of Schmidt et al. [27]. Firstly, the 5 wt% Nafion solution was diluted 10 times in deionized water. Then, 0.008 g of the powder was added to 1 cm³ of water and 0.20 cm³ of the diluted Nafion[®] solution. The resulting system was placed in an ultrasonic bath for 3 min to disperse the powder in the solution. Finally, 0.02 cm³ of the obtained dispersion were transferred onto a BDD electrode with geometric area of 0.125 cm². The deposited suspension was then dried for 60 min at 80 °C to complete evaporation of the solvents, thereby obtaining a thin layer of the catalyst powder fixed onto the diamond electrode.

3. Results and discussion

3.1. Structure and composition of the Pt–RuO₂/C composite

Fig. 1 shows the X-ray diffraction (XRD) pattern for the composite containing Pt, Ru and C and prepared by the sol–gel technique. The presence of polycrystalline Pt (JCPDS #04-0802) is revealed by the peaks in 2θ values at around 39, 46 and 67°. The corresponding crystal planes are (1 1 1), (2 0 0) and (2 2 0), respectively, and are in agreement with previous results for the

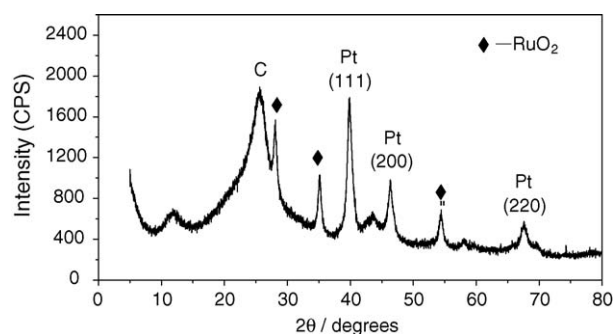


Fig. 1. XRD pattern taken at 2° min⁻¹ for the Pt–RuO₂/C composite. The peaks marked with (◆) reveal the RuO₂ presence in the sample. The different peaks for polycrystalline Pt and the carbon presence are directly indicated in the graph.

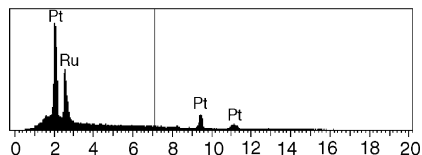


Fig. 2. EDX spectrum for the Pt–RuO₂/C composite. The carbon response was omitted, due to the very intense signal if compared to the metals. The quantitative analysis revealed that the proportion of metals on the sample was approximately 50–50% of Pt and Ru.

synthesis of similar powder composites using different deposition techniques [28,29].

The Bragg angles marked with (◆) in Fig. 1 are related to RuO₂ [30] (JCPDS #43-1027) but the experimental results show a small shift of Bragg angles toward higher values with respect to the expected ones. These shifts are a consequence of some degree of Pt–RuO₂ alloying [31], which is probably resulting from the sol–gel deposition technique. The average size of crystallites has been calculated as being 7.2 nm using the WinFit 1.2 software and the Scherrer relationship. Although the calculated value is just an approximation, it has been shown in previous studies that the present estimate is in good agreement with the particle size determined by Transmission Electron Microscopy (TEM) [32,33]. Moreover, such small value indicates that the sol–gel technique is very adequate for producing nano-structured catalysts.

Fig. 2 shows the EDX spectrum of the Pt–RuO₂/C composite after suppressing the signal due to carbon. The platinum and ruthenium values taken as an average of three different points of the sample are 50.4 and 49.6% (w/w), respectively. The measured Pt/Ru ratio is in very close agreement with that used in the sol–gel preparation of the composite.

3.2. Catalytic properties of the Pt–RuO₂/C composite supported on BDD

Initial electrochemical tests were carried out to compare the response of the Pt–RuO₂/C composite fixed on either BDD or glassy carbon (GC). The cyclic voltammetric responses for both configurations recorded at 10 mV s⁻¹ in a 1.0 mol dm⁻³ CH₃OH + 0.5 mol dm⁻³ H₂SO₄ solution are presented in Fig. 3. To allow a proper comparison with literature values, current densities were calculated in terms of the amount of Pt in the catalyst sample. The insert of Fig. 3 clearly shows that the capacity in the potential range 100–400 mV versus HESS for GC (1.26×10^{-5} C) is considerably larger than that of BDD (2.69×10^{-6} C) thus partially justifying the better performance when using the BDD substrate. In the potential region of methanol oxidation, Fig. 3 shows that the Pt–RuO₂/C composite on the BDD substrate presents a higher current density than the same system on GC for both the forward and reverse scans as well as for the peak. Thus, at the specific potential of 720 mV versus HESS, this value is 16% higher for the first configuration.

On the other hand, an interesting difference is observed between the two complete voltammograms of Fig. 3 since for the BDD substrate the forward and backward lines are almost

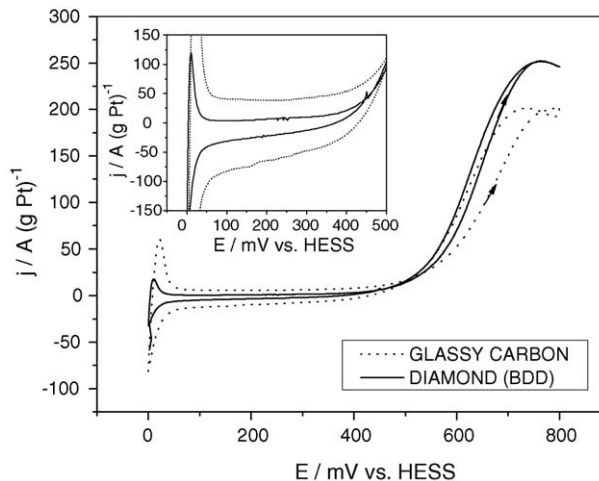


Fig. 3. Cyclic voltammetric responses of the Pt–RuO₂/C composite fixed on boron-doped diamond (full line) and on glassy carbon (dotted line) for the oxidation of 1.0 mol dm⁻³ methanol in 0.5 mol dm⁻³ H₂SO₄. The insert shows the region of capacitive responses for both electrode configurations, $\nu = 10 \text{ mV s}^{-1}$.

coincident while a large difference is observed for the GC case. Since both tests used the same Pt–RuO₂/C catalyst, the differences should be attributed to the substrate and probably reflect the larger capacitive effect of the GC already discussed. Therefore, in addition to the larger oxidation currents, the use of BDD practically eliminates the substrate contribution and the response of the electrode is only dependent on the catalyst.

Methanol and ethanol oxidation responses for the Pt–RuO₂/C catalyst on BDD can be observed in the cyclic voltammetric studies at 10 mV s⁻¹ presented in Fig. 4(a and b), respectively. Also included in those figures are the responses of a commercial 10% Pt/C catalyst on BDD, for comparison. The electrochemical responses of the blank solution are also included in those figures and show that in the potential range from 0.05 to 100 mV versus HESS a small signal for the Pt–H desorption and adsorption process is observed. This is probably due to the inhibitory presence of ruthenium on the platinum surface while no other faradaic processes can be detected outside that potential range.

The oxidation of methanol (Fig. 4(a)) starts at approximately 380 mV versus HESS for both materials and these results are in close agreement with previous ones obtained using a Pt–Ru/C composite synthesized using carbon nanotube as substrate [34]. It is also worth noticing that the current density values in the forward and backward scans of the voltammogram for the Pt–RuO₂/C composite are larger than those of the Pt/C commercial powder and very close to each other. This suggests the absence of an inhibitory or poisoning effect by adsorbed CO in the former case possibly due to the effective incorporation of RuO₂ by the sol–gel technique. Meanwhile, these assumptions will require further investigations.

In the case of ethanol oxidation (Fig. 4(b)), the responses for both materials are quite different and more complex than in the previous case. Thus, both materials revealed the presence of a re-activation process on the catalyst surface but for the Pt–RuO₂/C

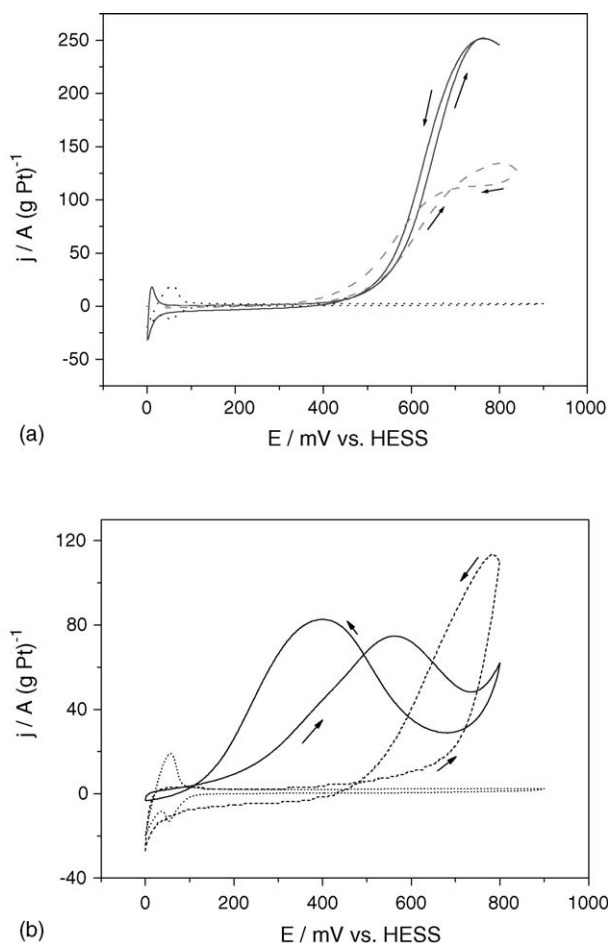


Fig. 4. Voltammetric oxidation of methanol (a) and ethanol (b) 1.0 mol dm^{-3} in $0.5 \text{ mol dm}^{-3} \text{ H}_2\text{SO}_4$ on Pt–RuO₂/C (full lines) and Pt/C (traced lines) composites fixed on BDD. The baselines (dotted lines) are also included for comparison, $\nu = 10 \text{ mV s}^{-1}$.

composite the oxidation of ethanol starts at much lower potentials than for the Pt/C powder. Moreover, the current density for the composite remains fairly large for an extended potentials interval indicating a multi-step process as well as an expressive oxidation of the intermediates in the backward scan of the cyclic voltammogram.

A very convenient way of comparing the performance of different electrode materials for a given process is the use of steady-state polarization curves and the corresponding Tafel plots. This innovative procedure allows a clear and pictorial view of two important parameters, namely the starting potential and the current density value for the systems under investigation. Thus, Fig. 5 shows the Tafel plots carried out in the potentiostatic mode for methanol and ethanol oxidation processes on both materials (Pt–RuO₂/C and Pt/C) fixed on BDD and using the same electrolyte solutions as before.

It is clear from Fig. 5 that the Pt–RuO₂/C composite has a better performance than Pt/C regarding starting oxidation potentials and current densities. For methanol oxidation on the composite, the Tafel plot has a slope (b) of ca. 120 mV dec^{-1} . In a recent investigation under similar experimental conditions but using a commercial Pt–Ru/C powder, a value 124 mV dec^{-1} was

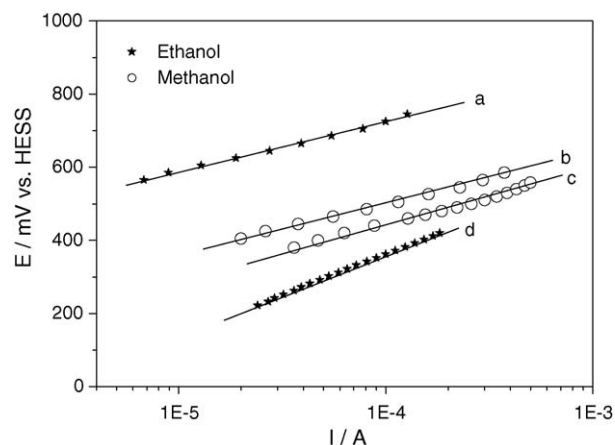
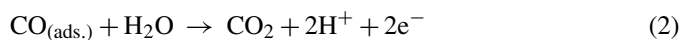
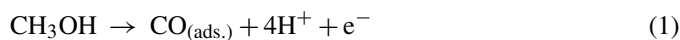


Fig. 5. Tafel plots recorded in the galvanostatic mode for $0.5 \text{ mol dm}^{-3} \text{ CH}_3\text{OH}$ (circles) and $0.5 \text{ mol dm}^{-3} \text{ CH}_3\text{CH}_2\text{OH}$ (stars) oxidation in $0.5 \text{ mol dm}^{-3} \text{ H}_2\text{SO}_4$ on Pt/C (curves a and b) and Pt–RuO₂/C (curves c and d) composites fixed on BDD.

reported for methanol oxidation in acid medium and the following mechanism was proposed [35]:



Assuming that the first electron transfer (Eq. (1)) is the rate-determining step, the expected theoretical value for b should be 118 mV dec^{-1} [35], in very close agreement with the experimental value determined here.

For the oxidation of ethanol on the Pt–RuO₂/C composite electrode the b value is ca. 140 mV dec^{-1} . However, in this case the existing mechanism is extremely complex [36] and still requires further experimental evidences to allow for the establishment of the *rds* thus allowing for theoretical calculations of the Tafel slope value (b).

Chronoamperometric experiments were carried out to observe the stability and possible poisoning of the catalysts under short-time continuous operation. Fig. 6 shows the current–time curves recorded for the two electrode systems in $1.0 \text{ mol dm}^{-3} \text{ CH}_3\text{OH}$ or $\text{CH}_3\text{CH}_2\text{OH}$ and $0.5 \text{ mol dm}^{-3} \text{ H}_2\text{SO}_4$ solutions at a fixed potential of 550 mV versus HESS. As expected, a fast decay was observed at the beginning of the oxidation process while a slower one was observed for the rest of the experiment. Meanwhile, that initial decay was much less pronounced in the case of ethanol for both the Pt–RuO₂/C composite and the Pt/C powder thus suggesting that poisoning of the electrode surface is less important for ethanol oxidation.

Slow and continuous current decays have also been observed by other authors when Pt–Ru systems were studied and different mechanisms were proposed [37]. It was assumed that either both decays are related to the presence of impurities in the solution or that the fast decay is related to the formation of superior oxides while the slow one is due to the poisoning of the material during the advance of process [38].

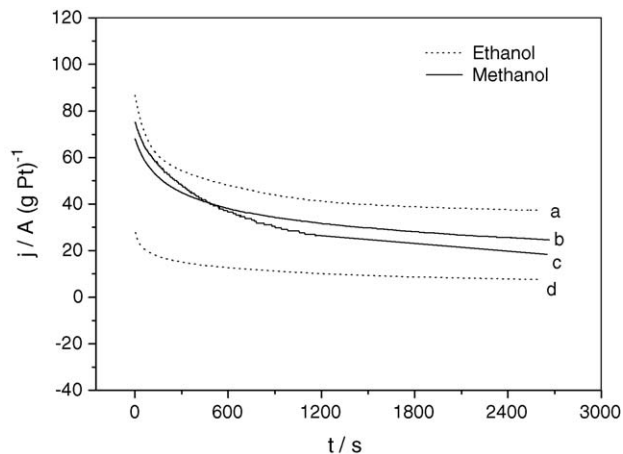


Fig. 6. Current–time responses measured at 550 mV vs. HESS for 0.5 mol dm^{-3} CH_3OH (full lines) and 0.5 mol dm^{-3} $\text{CH}_3\text{CH}_2\text{OH}$ (dotted lines) oxidation in 0.5 mol dm^{-3} H_2SO_4 on Pt/C (curves a and b) and Pt–RuO₂/C (curves c and d) composites fixed on BDD.

4. Conclusions

The preparation of the Pt–RuO₂/C composite by the sol–gel technique rendered a very efficient electrocatalyst for both methanol and ethanol oxidation in acid medium when compared to a commercially available Pt/C powder. This was reflected by the initial potentials for the processes and the enhanced current densities as well as by a lower degree of poisoning by undesired intermediates, probably CO.

Moreover, the sol–gel technique produced homogeneous and nanosized crystalline particles of the desired composition in a rather simple and straightforward manner. These advantages of the technique could become very important when the preparation of large amounts of catalyst powders would be required for fuel cells manufacturing.

On the other hand, the use of a boron-doped diamond electrode as the substrate of the catalysts powders proved to be more efficient than other materials such as glassy carbon, an effect that could be attributed to the lower capacity currents shown by the BDD and perhaps to a better distribution of the powder on their surface.

Acknowledgements

To FAPESP (Proc. 01/14320-0), CAPES (Proc. BEX 0800/03-1) and CNPq, Brazil, for the scholarships and financial support to this work.

References

[1] Z. Jusys, R.J. Behm, *Electrochim. Acta* 49 (2004) 3891–3900.
 [2] L. Xiong, A. Manthiram, *Electrochim. Acta* 49 (2004) 4163–4170.
 [3] E.V. Spinacè, A.O. Neto, M. Linardi, *J. Power Sources* 129 (2004) 121–126.
 [4] Y. Takasu, T. Kawaguchi, W. Sugimoto, Y. Murakami, *Electrochim. Acta* 48 (2003) 3861–3868.

[5] K.W. Park, B.K. Kwon, J.H. Choi, I.S. Park, Y.M. Kim, Y.E. Sung, *J. Power Sources* 109 (2002) 439–445.
 [6] A.K. Shukla, R.K. Raman, N.A. Choudhury, K.R. Priolkar, P.R. Sarode, S. Emura, R. Kumashiro, *J. Electroanal. Chem.* 563 (2004) 181–190.
 [7] E.V. Spinacè, A.O. Neto, T.R.R. Vasconcelos, M. Linardi, *J. Power Sources* 137 (2004) 17–23.
 [8] W. Zhou, Z. Zhou, S. Song, W. Li, G. Sun, P. Tsiakaras, Q. Xin, *Appl. Catal. B: Environ.* 46 (2003) 273–285.
 [9] L. Gao, H. Huang, C. Korzeniewski, *Electrochim. Acta* 49 (2004) 1281–1287.
 [10] S.Lj. Gojkovic, T.R. Vidakovic, D.R. Durovic, *Electrochim. Acta* 48 (2003) 3607–3614.
 [11] T. Okada, Y. Suzuki, T. Hirose, T. Ozawa, *Electrochim. Acta* 49 (2004) 385–395.
 [12] M. Umeda, M. Kokubo, M. Mohamedi, I. Uchida, *Electrochim. Acta* 48 (2003) 1367–1374.
 [13] A. Oliveira Neto, E.G. Franco, E. Aricó, M. Linardi, E.R. Gonzalez, *J. European Ceram. Soc.* 23 (2003) 2987–2992.
 [14] H. Bönemann, W. Brijoux, R. Brinkmann, E. Dinjus, R. Fretzen, T. Joußen, B. Korall, *J. Mol. Cat.* 74 (1992) 323–333.
 [15] H.B. Suffredini, J.L. Cerne, F. Crnkovic, S.A.S. Machado, L.A. Avaca, *Int. J. Hydrogen Energy* 25 (2000) 415–423.
 [16] M. Fallet, H. Mahdjoub, B. Gautier, J.P. Bauer, *J. Non-Crystalline Sol.* 293 (2001) 527–533.
 [17] F. Perdomo L., P. de Lima-Neto, M.A. Aegerter, L.A. Avaca, *J. Sol–Gel Sci. Techn.* 15 (1999) 87–91.
 [18] H.B. Suffredini, V. Tricoli, L.A. Avaca, N. Vatisstas, *Electrochem. Comm.* 6 (2004) 1025–1028.
 [19] F. Montilla, E. Morallón, I. Duo, Ch. Comninellis, J.L. Vázquez, *Electrochim. Acta* 48 (2003) 3891–3897.
 [20] G.M. Swain, *J. Electrochem. Soc.* 141 (1994) 3382–3393.
 [21] P.K. Bachmann, R. Messier, *Chem. Eng. News* 67 (1989) 24–27.
 [22] H.B. Suffredini, S.A.S. Machado, L.A. Avaca, *J. Braz. Chem. Soc.* 15 (2004) 16–21.
 [23] L.F. Li, D.A. Totir, B. Miller, G. Chottiner, A. Argoitia, J.C. Angus, D.A. Scherson, *J. Am. Chem. Soc.* 119 (1997) 7875–7876.
 [24] A. Perret, W. Haenni, P. Niedermann, N. Skinner, C. Comninellis, D. Gandini, *Electrochem. Soc. Proc.* 97 (1997) 275.
 [25] G.M. Swain, *Adv. Mater.* 6 (1994) 388–392.
 [26] H.B. Suffredini, V.A. Pedrosa, L. Codognoto, S.A.S. Machado, R.C. Rocha-Filho, L.A. Avaca, *Electrochim. Acta* 49 (2004) 4021–4026.
 [27] T.J. Schmidt, H.A. Gasteiger, G.D. Stab, P.M. Urban, D.M. Kolb, R.J. Behm, *J. Electrochem. Soc.* 145 (1998) 2354–2357.
 [28] M.S. Löffler, H. Natter, R. Hempelmann, K. Wippermann, *Electrochim. Acta* 48 (2003) 3047–3051.
 [29] J. Prabhuram, T.S. Zhao, C.W. Wong, J.W. Guo, *J. Power Sources* 134 (2004) 1–6.
 [30] J. Pagnaer, D. Nelis, D. Mondelaers, G. Vanhoyland, J. D’Haen, M.K. Van Bael, H. Van den Rul, J. Mullens, L.C. Van Poucke, *J. European Ceram. Soc.* 24 (2004) 919–923.
 [31] J.M. Qian, J.P. Wang, G.J. Qiao, Z.H. Jin, *J. European Ceram. Soc.* 24 (2004) 3251–3259.
 [32] A.S. Aricó, P. Cretì, P.L. Antonucci, J. Cho, H. Kim, V. Antonucci, *Electrochim. Acta* 43 (1998) 3719–3729.
 [33] W.J. Zhou, B. Zhou, W.Z. Li, Z.H. Zhou, S.Q. Song, G.Q. Sun, Q. Xin, S. Douvartzides, M. Goula, P. Tsiakaras, *J. Power Sources* 126 (2004) 16–22.
 [34] Z. He, J. Chen, D. Liu, H. Zhou, Y. Kuang, *Diamond Relat. Mater.* 13 (2004) 1764–1770.
 [35] G. Wu, L. Li, B.Q. Xu, *Electrochim. Acta* 50 (2004) 1–10.
 [36] A. Oliveira-Neto, M.J. Giz, J. Perez, E.A. Ticianelli, E.R. Gonzalez, *J. Electrochem. Soc.* 149 (2002) A272–A279.
 [37] H. Gasteiger, N. Marcovi, P. Ross, E. Cairns, *J. Electrochem. Soc.* 141 (1994) 1795–1803.
 [38] H. Hoster, T. Iwasita, H. Baumgartner, W. Vielstich, *J. Electrochem. Soc.* 148 (2001) A496.